Rarefaction and Non-equilibrium Effects in Hypersonic Flows about Leading Edges of Small Bluntness

Mikhail Ivanov[a], Dmitry Khotyanovsky[a], Alexey Kudryavtsev[a], Anton Shershnev[a], Yevgeniy Bondar[a], Shigeru Yonemura[b]

[a]*Khristianovich Institute of Theoretical and Applied Mechanics SB RAS, 4/1 Institutskaya str., Novosibirsk 630090, Russia*
[b]*Institute of Fluid Science, Tohoku University, Katahira 2-1-1, Aoba-ku, Sendai, Japan 980-8577*

Abstract. A hypersonic flow about a cylindrically blunted thick plate at a zero angle of attack is numerically studied with the kinetic (DSMC) and continuum (Navier-Stokes equations) approaches. The Navier-Stokes equations with velocity slip and temperature jump boundary conditions correctly predict the flow fields and surface parameters for values of the Knudsen number (based on the radius of leading edge curvature) smaller than 0.1. The results of computations demonstrate significant effects of the entropy layer on the boundary layer characteristics.

Keywords: leading edge, hypersonic boundary layer, rarefaction effects
PACS: 51.10.+y

INTRODUCTION

Leading edges of small bluntness can be used as elements of advanced spacecraft and hypersonic aircraft design to provide a high lift-to-drag ratio. A specific feature of the high-speed flow about such edges is a significant local effect of rarefaction and thermal non-equilibrium even for segments of the flight trajectory where the flow about the vehicle is not rarefied as a whole. Because of difficulties in experimental modeling of such flows, an important task is the development of an efficient approach for correct simulation of high-speed flows near leading edges.

The leading edge area may affect the flow at large downstream distances even if rarefaction effects in the vicinity of the leading edge are insignificant. The flow passing through the near-normal bow shock detached from the blunted leading edge causes formation of an inviscid entropy layer near the body. Farther downstream, the entropy layer is swallowed by the growing viscous boundary layer. Entropy/boundary layer interaction causes significant changes in boundary layer characteristics. In particular, the entropy layer greatly affects the boundary layer stability. At small bluntness, the laminar/turbulent transition point is displaced downstream. Greater bluntness produces a *boundary layer transition reversal*, i.e. additional blunting produces forward displacement of the transition point. The swallowing distance of the entropy layer is an important correlation parameter for the transition reversal [1]. If the rarefaction effects are significant, the flow pattern in the vicinity of the blunted leading edge becomes more complicated: in particular, a merged layer can be observed (as in the case of a sharp leading edge on a flat plate, see, e.g., [2]), where it is impossible to distinguish the shock wave, entropy layer, and boundary layer. In this case, the velocity distribution function may be substantially nonequilibrium; in addition, translational-rotational and translational-vibrational nonequilibrium may be observed. The role of these processes in the vicinity of the leading edge on boundary layer development is not fully understood.

The parameter that characterizes the rarefaction and thermal non-equilibrium effects is the Knudsen number based on the leading edge radius of curvature $\mathrm{Kn}_C=\lambda/R_C$. When the Knudsen number is of the order of 0.01 or lower, the continuum approach and traditional methods of computational fluid dynamics based on the Navier-Stokes (NS) equations are usually used. For higher Knudsen numbers up to 0.1, the NS equations should be used with taking into account the initial rarefaction effects through the velocity slip and temperature jump boundary conditions [3]. For Knudsen numbers higher than 0.1, the kinetic approach based on the solution of the Boltzmann equation is usually

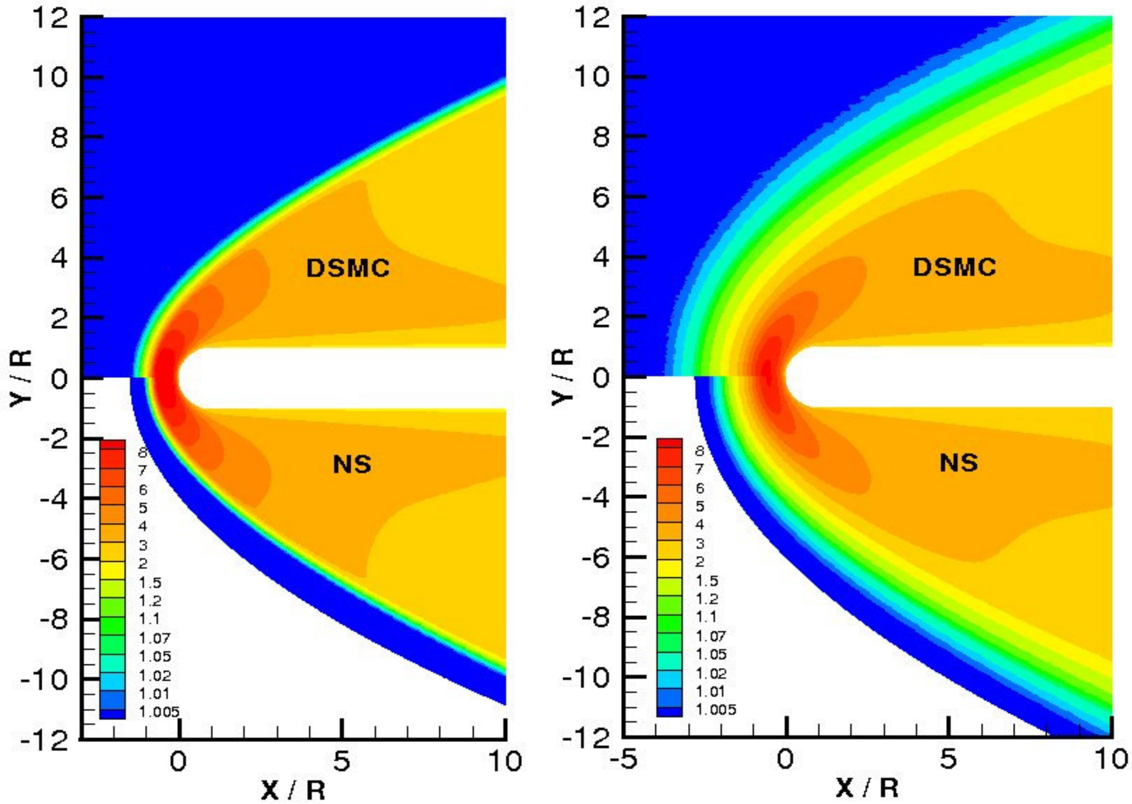

FIGURE 1. Temperature flowfields for M=5, $Kn_R = 0.1$ (left) and $Kn_R = 0.5$ (right).

employed. The most efficient numerical technique for solving the Boltzmann equation for high-speed flows is the Direct Simulation Monte Carlo (DSMC) method [4].

Numerical studies of hypersonic flows about blunted leading edges are performed in the present work on the basis of the kinetic (DSMC) and continuum (NS equations) approaches. The use of such a combined numerical strategy allows us to investigate the rarefaction and thermal nonequilibrium effects in the vicinity of the leading edge and to assess the area of applicability of the continuum approach. Attention is also paid to development of the entropy layer and its interaction with the boundary layer at Kn_c close to the boundary of applicability of the continuum approach.

NUMERICAL TECHNIQUES

Computations of M=5 and M=10 flows of a monatomic gas near the leading edge of a cylindrically blunted thick plate at a zero angle of attack was conducted by both NS and DSMC codes for the Knudsen numbers Kn_C=0.1 - 0.5 (the geometry is shown in Fig.1). The plate length is $10R_c$. Note that the Knudsen number based on the plate length is within the range Kn~0.01-0.05, which is believed to be within the area of applicability of the NS equations. A time-explicit shock-capturing code based on a 4th order MUSCL TVD scheme for convective terms and a second-order central difference approximation of diffusive terms were used for solving the NS equations with the velocity slip and temperature jump boundary conditions [3]:

$$u_s = \alpha_u \lambda \left(\frac{\partial u}{\partial y} \right)_s , \qquad T_s - T_w = \alpha_T \frac{\gamma}{\gamma - 1} \frac{\lambda}{\Pr} \left(\frac{\partial T}{\partial y} \right)_s .$$

Here the subscript s refers to the gas quantities near the wall, u is the velocity component tangential to the wall and T_w is the wall temperature. These boundary conditions can be deduced from an approximate solution of the kinetic equation in the Knudsen layer assuming the diffusive reflection of molecules from the wall with complete accommodation. The calculation gives for the numerical values of coefficients $\alpha_u = 1.142$ and $\alpha_T = 0.5865$.

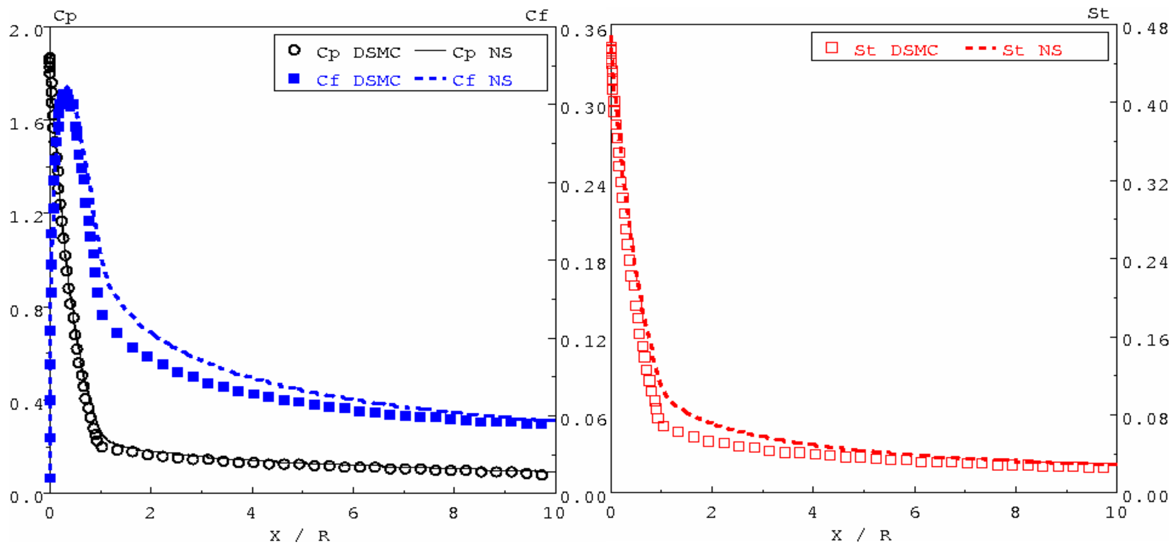

FIGURE 2. Surface parameters for M=5, $Kn_R = 0.5$.

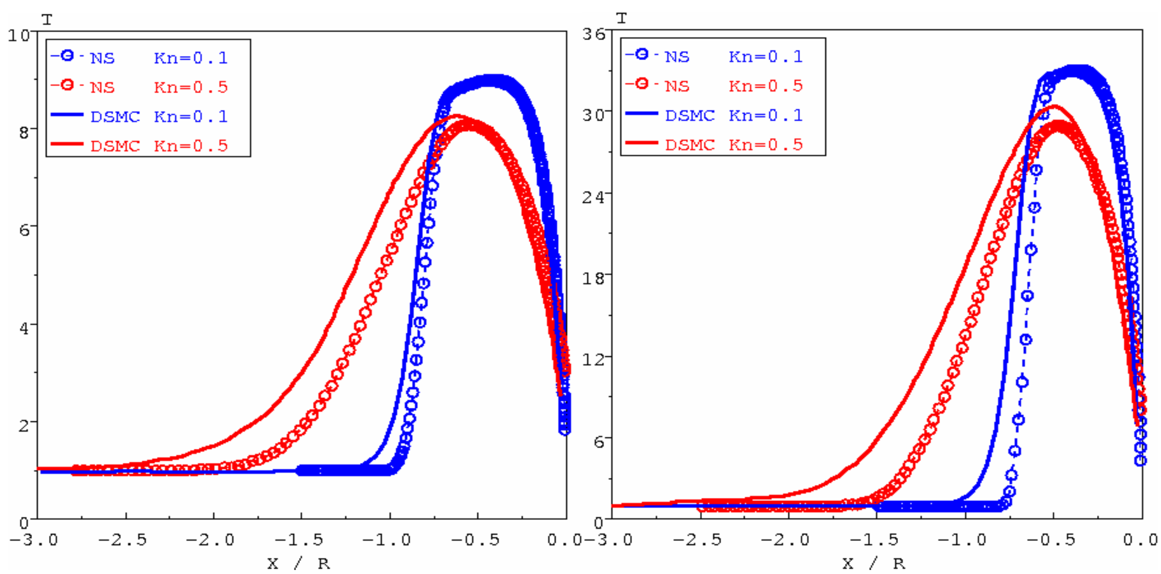

FIGURE 3. Temperature along the stagnation streamline for M=5 (left) and M=10 (right).

DSMC computations were performed with the SMILE software system [5]. The plate was assumed to be isothermal with the temperature equal to the free-stream value. A diffuse reflection model with complete energy accommodation was used in the DSMC computations. The hard sphere collision model used in the DSMC simulations was consistent with the square root viscosity-temperature dependence in the NS computations.

RESULTS

The distribution of the pressure coefficient C_p, friction coefficient C_f, and Stanton number St over the plate surface for the Knudsen number Kn_c=0.5 is given in Fig. 2. For this Knudsen number, the kinetic and continuum approaches predict similar distributions of all parameters, namely, dimensionless pressure, friction, and heat flux. The NS friction coefficient values are more than 10 % greater than the DSMC values in some parts of the surface. The heat flux obtained in the NS computations is also higher than that predicted by the DSMC method (by more than 20 % for some parts of the surface). The results predicted by different approaches become closer to each other as the Knudsen number decreases. The pattern observed at the higher Mach number (M=10) is qualitatively similar.

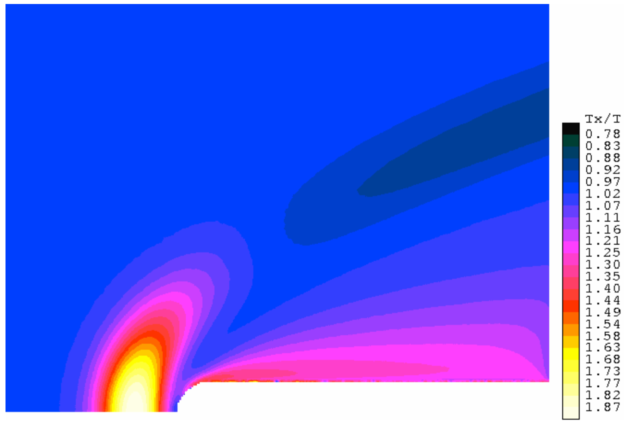

FIGURE 4. T_x/T flowfield (DSMC, M=10, Kn_c=0.5).

As a whole, the NS equations with slip boundary conditions ensure a correct result (i.e. NS surface distributions are very close to DSMC ones) for Kn_c=0.1 and lower.

The temperature flowfields are shown in Fig. 1 for M=5 and different Knudsen numbers. Though the NS and DSMC isolines in the area behind the bow shock are similar for both Knudsen numbers, a significant difference is observed in the shock wave thickness, which is much higher for the DSMC flowfield, especially for the higher Knudsen number. For M=10, the results are similar. An internal structure of the shock wave is seen in more detail in Fig. 3, which shows the temperature along the stagnation line for different Mach and Knudsen numbers. The behavior of the temperature profiles is qualitatively identical for different Mach numbers. For Kn_c=0.1, the flow along the stagnation line can be divided into the free stream, shock wave, region directly behind the shock wave with a moderate temperature gradient (viscous shock layer), and boundary layer directly adjacent to the stagnation point. The difference between the continuum and kinetic approaches is observed only inside the shock wave front (the DSMC method predicts a thicker wave than the NS equations). At the higher Knudsen number Kn_c=0.5, a merged layer is formed, the shock wave merges with the boundary layer, and the kinetic approach predicts a significantly greater wave thickness than the continuum approach (NS). The flow in the merged layer is substantially nonequilibrium. Figure 4 shows the field of dimensionless temperature (ratio of the temperature in the x direction to the total temperature, which is a parameter characterizing the anisotropy of the velocity distribution function). For Kn_c=0.5, the distribution function is substantially nonequilibrium almost in the entire flowfield in the vicinity of the leading edge, which is caused by the presence of a thick shock wave and also by violation of equilibrium in the flow near a cold wall.

In the case considered, we cannot speak about the inviscid entropy layer, because the flow behind the bow shock wave front is nonequilibrium and viscous (at the higher Knudsen number, the viscous shock wave front and the boundary layer even merge together). At the smaller Knudsen number, the process of entropy layer formation is demonstrated in Fig. 5, where the flowfields and the profiles of parameters for the blunted plate with Kn_c=0.1 and for the sharp plate are compared. Plate bluntness leads to significant amplification of the shock wave, which is manifested, in particular, in an increase in entropy and a decrease in the Mach number behind the front. The velocity profiles show that the boundary layer thicknesses in these two cases are close to each other, while the high entropy region is substantially wider in the case of the blunted plate. This fact demonstrates the presence of an entropy layer propagating downstream from the subsonic region ahead of the frontal part of the blunted plate. Note that a small increase in entropy is observed downstream in both cases, which is associated with viscous dissipation. There is a decrease in entropy in an immediate vicinity of the wall because of heat losses on the cold wall.

Figure 6 shows the streamwise velocity and entropy for different sections along x axis, which allow us to estimate the boundary layer evolution near the leading edge and its interaction with the entropy layer. At the smaller Knudsen number, the boundary layer is clearly seen as a region with a high gradient of velocity near the wall; with increasing y, there follows a constant velocity flow up to the shock wave where a high velocity gradient is again observed. At the higher Knudsen number, the boundary layer and the shock wave are rather weakly separated from each other at small distances from the edge; a plateau with a constant value of velocity at the boundary layer edge is formed only at X/R=10. The entropy curve is non-monotonic for both Knudsen numbers. At Kn_c=0.1, it has two peaks: one is the entropy maximum inside the shock wave, and the other peak is associated with the presence of the entropy layer. At the higher Knudsen number, the first peak is always observed, while the second peak is formed at some distance from the leading edge. The figures at larger downstream distances illustrate gradual swallowing of the entropy layer by the growing boundary layer. A more detailed study of this process should be performed on flat plates of considerably greater lengths.

SUMMARY AND CONCLUSIONS

A hypersonic flow around a blunted thick plate at a zero angle of attack in the transitional regime is numerically simulated by DSMC and Navier-Stokes solvers. It is demonstrated that the Navier-Stokes equations can be successfully used to describe the viscous flow behind the shock wave at Knudsen numbers based on the bluntness radius smaller than 0.1 is the initial rarefaction effects are taken into account through velocity slip and temperature jump boundary conditions on the plate surface. At Knudsen numbers about 0.5, the rarefaction effects are more noticeable; in particular, there is significant anisotropy of the distribution function, but the Navier-Stokes equations still yield a qualitatively correct result.

The emergence of the bow shock wave on a blunted plate leads to formation of an entropy layer, which cannot be considered as inviscid in the range of parameters considered. At Knudsen numbers about 0.5, the entropy layer is inside the merged layer, which is formed by merging of the shock wave and the boundary layer. At Knudsen numbers about 0.1, the shock wave is separated from the boundary layer. As the boundary layer grows, it swallows the entropy layer.

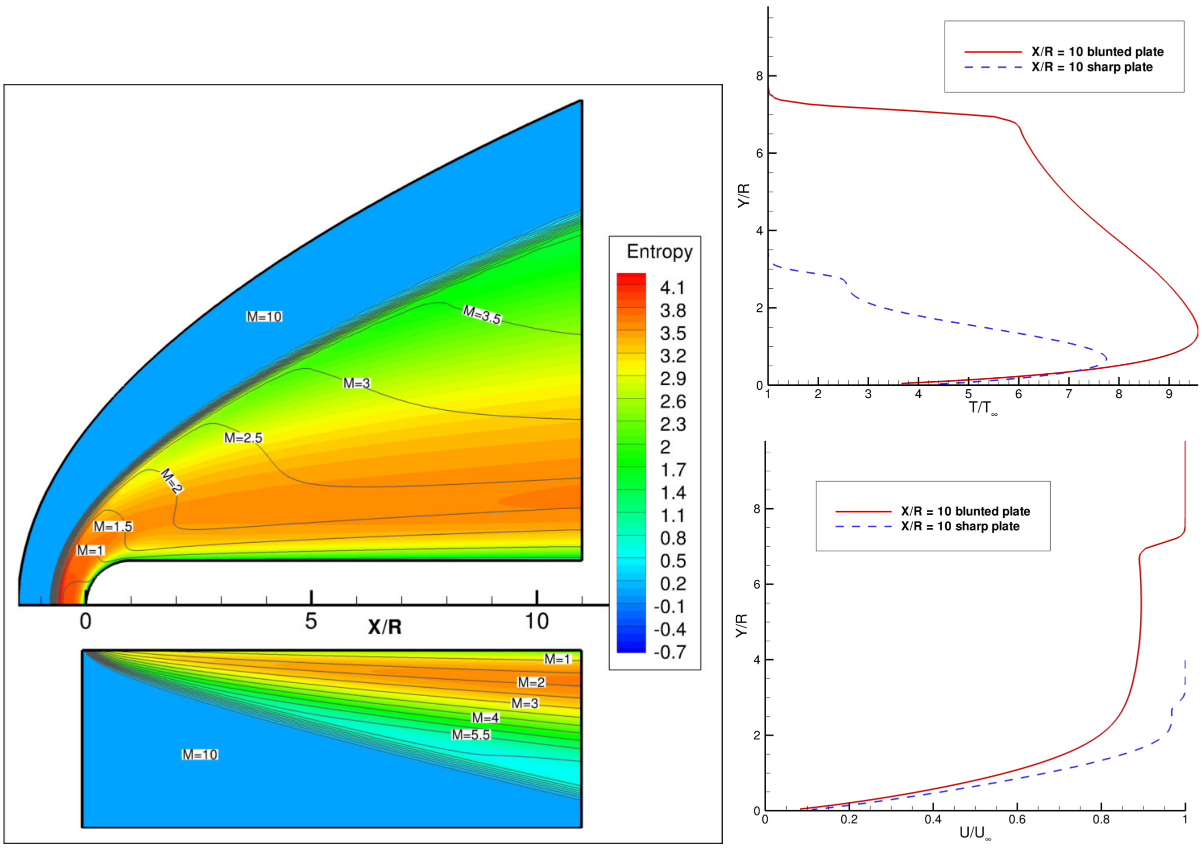

FIGURE 5. Entropy / Mach number flowfields and y-profiles of temperature and velocity for blunted and sharp plates (NS, M=10).

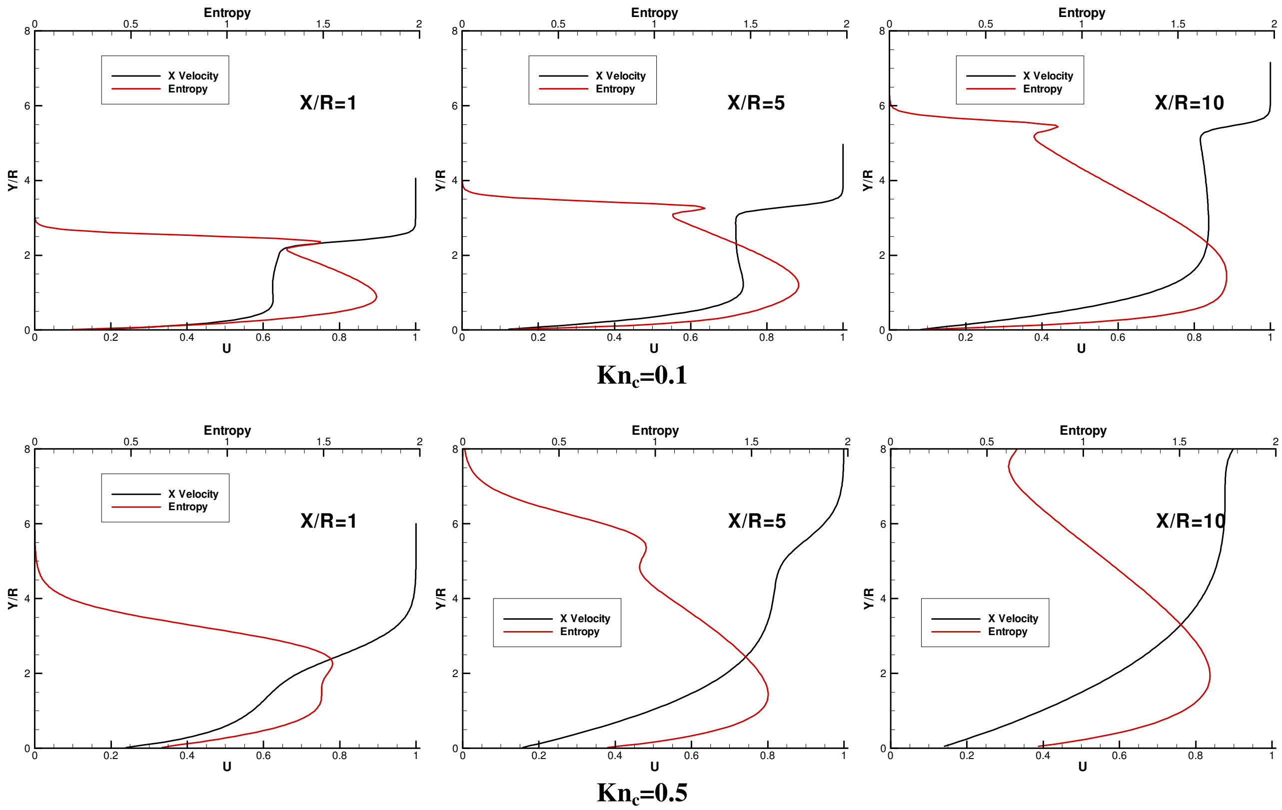

FIGURE 6. Entropy / Velocity y-profiles at different locations (NS, M=10).

ACKNOWLEDGMENTS

The present study is supported by the IFS Collaborative Research Project "Investigation of Hypersonic Flows about Leading Edges of Small Bluntness," Russian Foundation for Basic Research (RFBR Project No. 10-08-01203-a), Lavrentyev Youth Grant "High-altitude aerothermodynamics of advanced spacecraft taking into account non-equilibrium chemical reactions," and Program No. 11 of the Presidium of the Russian Academy of Sciences. This support is gratefully acknowledged.

REFERENCES

1. Stetson K.F., Rushton G.H. Shock tunnel investigation of the boundary layer transition at M = 5.5. *AIAA J.* 1967. Vol. 5. P. 899-906.
2. A. B. Huang and D.L. Hartley, Kinetic Theory of the Sharp Leading Edge Problem in Supersonic Flow, *Physics of Fluids,* Vol. 12, No.1, pp. 96-108, 1969.
3. M.N. Kogan, *Rarefied Gas Dynamics*. Plenum Press, 1969.
4. G.A.Bird. *Molecular Gas Dynamics and Direct Simulation of Gas Flows*. Clarendon Press: Oxford, 1994.
5. M.S. Ivanov, G.N. Markelov, S.F. Gimelshein. "Statistical Simulation of Reactive Rarefied Flows: Numerical Approach and Applications." AIAA Paper 98-2669 (1998).